

Joint Equalization and Decoding for Nonlinear Two-Dimensional Intersymbol Interference Channels

Naveen Singla and Joseph A. O'Sullivan
Department of Electrical & Systems Engineering
Washington University
St. Louis, MO 63130, USA
Email: [singla, jao]@wustl.edu

Abstract—An algorithm that performs joint equalization and decoding for channels with nonlinear two-dimensional intersymbol interference is presented. The algorithm performs sum-product message-passing on a factor graph that represents the underlying system. The two-dimensional optical storage (TwoDOS) technology is an example of a system with nonlinear two-dimensional intersymbol interference. Simulations for the nonlinear channel model of TwoDOS show significant improvement in performance over uncoded performance. Noise tolerance thresholds for the TwoDOS channel computed using density evolution are also presented.

I. INTRODUCTION

Two-dimensional (2D) intersymbol interference (ISI) channels have received a lot of attention lately. This is mainly due to the fact that research focus in the storage industry is shifting towards developing a two-dimensional paradigm for storage. Current storage technologies are restricted by physical limits which will prevent them from keeping up with the ever increasing demands for data storage. This has prompted the development of technologies that employ novel techniques for data storage. Patterned magnetic media, in which information is stored in isolated single grain islands, make areal densities of the order of 10^{12}bits/in^2 feasible, which is far beyond the limits of conventional magnetic recording. Holographic storage, page-oriented optical memories, and the two-dimensional optical storage (TwoDOS) technology are potential optical storage technologies of the future. Due to the two-dimensional nature of storage, these advanced storage technologies have 2D ISI during the readback process. Conventional recording technologies like magnetic hard disks and DVDs have one-dimensional ISI for which partial response maximum-likelihood decoding has been highly successful. Extending PRML to two dimensions is not straightforward since maximum-likelihood decoding in two-dimensions is computationally infeasible. This motivates the need for new methods to combat 2D ISI. Besides advanced storage technologies, multi-user communication scenarios, like cellular communication, also have situations where 2D ISI is prevalent.

Detection schemes for 2D ISI channels have been proposed by many researchers [1]-[5]. Singla *et al.*, [6], [7] have proposed joint equalization and decoding schemes for 2D ISI channels and have shown the benefit of using error-correction coding in conjunction with detection. More often than not, the ISI is modeled as a linear filter. Although a good starting point,

the linearity assumption doesn't hold in general. TwoDOS is an example of a system where the ISI is nonlinear.

TwoDOS is, potentially, the next generation optical storage technology with projected storage capacity twice that of the blu-ray disk and with ten times faster data access rates [8], [9]. As in conventional optical disk recording, bits in the TwoDOS model are written on the disk in spiral tracks. However, instead of having a single row of bit cells, each track consists of a number of bit rows stacked together. Thus, TwoDOS is a truly two-dimensional storage paradigm. Successive tracks on the disk are separated by a guard band which consists of one empty bit row. In addition, the bit cells are hexagonal; this allows 15 percent higher packing density than rectangular bit cells leading to higher storage capacity. As in conventional optical disk recording, a 0/1 is represented by the absence/presence of a pit on the disk surface. A scalar diffraction model proposed by Coene [8] for optical recording is used to model the readback signal from the disk. Under this model the readback intensity from the disk has linear and bilinear contributions from the stored data.

Various detection schemes for TwoDOS have been proposed [9]-[11]. These schemes, with the exception of that proposed by Immink *et al.*, [9], use two-dimensional partial response equalization to obtain a linear channel model for the ISI. Then, equalization methods like minimum mean-squared-error equalization, are used for detection on this linear channel model. Since partial response equalization leads to noise correlation there is an inherent loss associated with these schemes. Thus, it is prudent to search for decoding schemes that avoid partial response equalization and are designed taking into account the nonlinear structure of the ISI. Immink *et al.*, [9] propose using a stripe-wise Viterbi detector that is designed for the nonlinear ISI. However, they did not employ any error correction coding.

In this paper, a low-complexity scheme for joint equalization and decoding for nonlinear 2D ISI channels is presented. The scheme was first proposed for linear 2D ISI channels [6] and has been appropriately modified for the nonlinear channel. This scheme, called the full graph scheme, performs sum-product message-passing on a joint graph that represents the error-correction code and the nonlinear 2D ISI channel. Low-density parity-check (LDPC) codes [12] are used for error correction. Simulations for the nonlinear channel model of

TwoDOS demonstrate the potential of using the full graph scheme. Significant improvement in performance is observed over uncoded performance. Noise tolerance thresholds are calculated for regular LDPC codes of different rates and full graph decoding for the nonlinear 2D ISI channel.

The paper is organized as follows. The model of the system and the channel model for TwoDOS is described in Section II. The full graph message-passing algorithm and its performance for TwoDOS are presented in Section III. The density evolution algorithm and the noise tolerance thresholds are presented in Section IV. Section V concludes the paper.

II. SYSTEM MODEL

The system is modeled as a discrete-time communication system governed by the following equation;

$$r(i, j) = h(\{x(k, l) : (k, l) \in \mathcal{N}_{ij}\}) + w(i, j). \quad (1)$$

Here, $r(i, j)$ is the data received at the output of the channel. $x(k, l)$ are the channel inputs, obtained by encoding the user data using an error correction code. The user data and the encoded data are assumed to be binary. LDPC codes are used for error correction. $w(i, j)$ are samples of additive white Gaussian noise (AWGN) with zero mean and variance σ^2 . \mathcal{N}_{ij} is the set of indices of all the bits that interfere with $x(i, j)$ during readback and $h(\cdot)$ is the function that encapsulates the nonlinear 2D interference.

For TwoDOS, a scalar diffraction model proposed by Coene [8] for optical recording is used to model the readback signal. Using the model, the readback signal (optical intensity) from the disk is

$$r(i, j) = 1 - \sum_{(k, l)} c(k, l)x(k, l) + \sum_{(k, l) \neq (m, n)} d(k, l; m, n)x(k, l)x(m, n), \quad (2)$$

where $c(k, l)$ and $d(k, l; m, n)$ are respectively the linear and nonlinear ISI coefficients. These coefficients depend on the parameters of the optical system, such as the wavelength of the laser, numerical aperture of the readback lens and geometry of the recording (pit and track dimensions). The extent of the interference is limited by the spot size of the laser used for reading. For low-to-moderate storage densities this leads to interference from the nearest neighbors only, whereas, for high storage densities (twice that of the blu-ray disk) the interference from bits in the other 'shells' also becomes significant [8].

Using a nearest neighbor interference model, the signal intensity in (2) depends on the data bit stored in the central bit cell and the 6 neighboring bit cells. If it is assumed that two configurations with the same central bit and same number of nonzero neighbors have identical signal values then the signal intensity takes on 14 values corresponding to the 14 different configurations. Fig. 1 shows four of these 14 configurations. As shown by Coene [8], this symmetry

assumption is a good approximation. Table I lists the signal levels for the 14 different configurations.



Fig. 1. Four of the possible 14 nearest neighbor configurations for TwoDOS. The dark circles in the cells depict a pit corresponding to a stored 1. Absence of a pit indicates a stored 0. The pits cover only about half the area of the hexagonal bit cells. This is done to reduce signal folding [8].

TABLE I

SIGNAL LEVELS FOR TWODOS RECORDING USING SCALAR DIFFRACTION MODEL AND NEAREST NEIGHBORS. (REPRODUCED FROM [8])

Nonzero neighbors (n)	Central bit=0 (s_{n_0})	Central bit=1 (s_{n_1})
0	0.95	0.50
1	0.80	0.35
2	0.70	0.30
3	0.55	0.20
4	0.45	0.15
5	0.35	0.10
6	0.25	0.05

This table is reproduced from [8] and corresponds to TwoDOS recording with hexagonal lattice parameter and pit-hole diameter equal to 165 nm and 120 nm, respectively. Using these parameters gives TwoDOS a 1.4 fold increase in storage density over the blu-ray disc. Looking at the table, the nonlinearity of the ISI is quite apparent; the signal level does not change linearly as the number of nonzero neighbors increases and the range when the central bit is a 0 is greater than when the central bit is 1. Similar to Immink *et al.*, [9] the signal levels in Table I take into account the interference from the outer shells (beyond the nearest neighbors) by taking an average across all the bit-patterns in these shells.

III. FULL GRAPH MESSAGE-PASSING ALGORITHM

The full graph algorithm computes approximate APPs of the codeword bits given the observations by performing message-passing on a factor graph representing the underlying system. This "full graph" has three types of nodes; variable nodes, check nodes, and measured data nodes corresponding to the codeword bits, the parity-check equations, and the observed data symbols, respectively. The upper two levels in the full graph represent the LDPC code bipartite graph showing how the codeword bits are connected to the check nodes via the LDPC code parity-check matrix. The lower two levels represent the channel ISI graph showing how the ISI induces dependencies between the codeword bits. Fig. 2 shows an illustration of the full graph where nearest neighbor interference is assumed.

Message-passing on this full graph is performed using the following schedule: variable nodes to check nodes, check nodes to variable nodes, variable nodes to measured data nodes and finally measured data nodes to variable nodes. Following is a brief description of how the messages are updated for each of

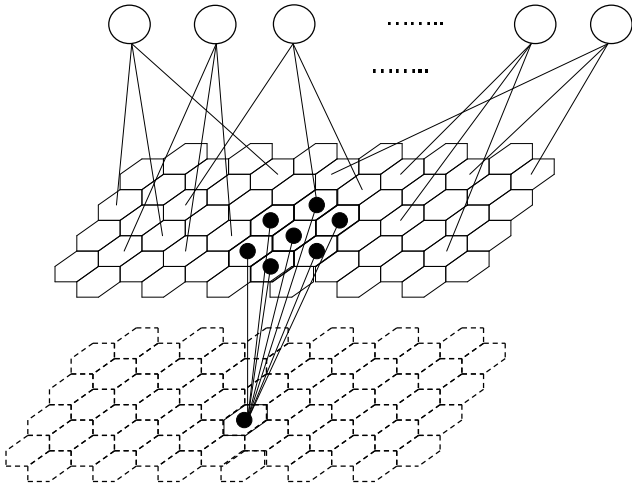


Fig. 2. Factor graph representation of the TwoDOS system.

the aforementioned four steps for the sum-product algorithm. The messages in the update equations are probabilities.

Variable-to-check messages: The message from a variable node x to a check node c at the l th iteration is calculated using the messages passed to x from its neighboring check and measured data nodes at the $(l-1)$ th iteration.

$$\begin{aligned}\mu_{x \rightarrow c}^{(l)}(0) &= \alpha \prod_{r \in N_r(x)} \mu_{r \rightarrow x}^{(l-1)}(0) \prod_{c' \in N_c(x) \setminus c} \mu_{c' \rightarrow x}^{(l-1)}(0) \\ \mu_{x \rightarrow c}^{(l)}(1) &= \alpha \prod_{r \in N_r(x)} \mu_{r \rightarrow x}^{(l-1)}(1) \prod_{c' \in N_c(x) \setminus c} \mu_{c' \rightarrow x}^{(l-1)}(1),\end{aligned}\quad (3)$$

where $\mu_{x \rightarrow c}^{(l)}(\cdot)$, $\mu_{r \rightarrow x}^{(l)}(\cdot)$, and $\mu_{c' \rightarrow x}^{(l)}(\cdot)$ are respectively, the variable-to-check, measured data-to-variable, and check-to-variable messages at the l th iteration. $N_c(x)$ and $N_r(x)$ are the neighboring check and measured data nodes of x respectively, and α is a normalizing constant.

Check-to-variable messages: At the l th iteration the check-to-variable messages are calculated using the variable-to-check messages at the l th iteration and the sum-product rule,

$$\begin{aligned}\mu_{c \rightarrow x}^{(l)}(0) &= \sum_{\{x': x' \in N(c) \setminus x\}} P(c|x=0, \{x'\}) \cdot \prod_{x' \in N(c) \setminus x} \mu_{x' \rightarrow c}^{(l)}(x') \\ \mu_{c \rightarrow x}^{(l)}(1) &= \sum_{\{x': x' \in N(c) \setminus x\}} P(c|x=1, \{x'\}) \cdot \prod_{x' \in N(c) \setminus x} \mu_{x' \rightarrow c}^{(l)}(x'),\end{aligned}\quad (4)$$

where $N(c)$ are the variable nodes connected to check node c .

Variable-to-measured data messages: The variable-to-measured data messages at the l th iteration are calculated using the messages received at the variable nodes from the check nodes at the l th iteration and from the measured data nodes at the $(l-1)$ th iteration,

$$\begin{aligned}\mu_{x \rightarrow r}^{(l)}(0) &= \alpha \prod_{c \in N_c(x)} \mu_{c \rightarrow x}^{(l)}(0) \prod_{r' \in N_r(x) \setminus r} \mu_{r' \rightarrow x}^{(l-1)}(0) \\ \mu_{x \rightarrow r}^{(l)}(1) &= \alpha \prod_{c \in N_c(x)} \mu_{c \rightarrow x}^{(l)}(1) \prod_{r' \in N_r(x) \setminus r} \mu_{r' \rightarrow x}^{(l-1)}(1).\end{aligned}\quad (5)$$

Measured data-to-variable messages: To complete one iteration, the measured data-to-variable messages at the l th iteration are computed using the variable-to-measured data messages at the l th iteration and the sum-product rule,

$$\begin{aligned}\mu_{r \rightarrow x}^{(l)}(0) &= \alpha \sum_{\{x': x' \in N(r) \setminus x\}} p(r|x=0, \{x'\}) \cdot \prod_{x' \in N(r) \setminus x} \mu_{x' \rightarrow r}^{(l)}(x') \\ \mu_{r \rightarrow x}^{(l)}(1) &= \alpha \sum_{\{x': x' \in N(r) \setminus x\}} p(r|x=1, \{x'\}) \cdot \prod_{x' \in N(r) \setminus x} \mu_{x' \rightarrow r}^{(l)}(x').\end{aligned}\quad (6)$$

$N(r)$ is the set of all variable nodes connected to measured data node r . The conditional probabilities above are values of a Gaussian probability density function. The mean of this probability density function is determined by the signal levels given in Table I and the variance is equal to the noise variance.

After this step the “pseudo-posterior” probabilities are calculated using the messages from the check nodes and the measured data nodes,

$$\begin{aligned}q_x^{(l)}(0) &= \alpha \prod_{r \in N_r(x)} \mu_{r \rightarrow x}^{(l)}(0) \prod_{c \in N_c(x)} \mu_{c \rightarrow x}^{(l)}(0) \\ q_x^{(l)}(1) &= \alpha \prod_{r \in N_r(x)} \mu_{r \rightarrow x}^{(l)}(1) \prod_{c \in N_c(x)} \mu_{c \rightarrow x}^{(l)}(1).\end{aligned}\quad (7)$$

The codeword estimate is obtained by setting \hat{x} to 1 if $q_x^{(l)}(1) > q_x^{(l)}(0)$ and 0 otherwise. The decoding stops if the decoder converges to a codeword or a maximum number of iterations is exhausted. The complexity of the full graph algorithm is linear in the LDPC code block length and quadratic in the size of the interfering neighborhood.

Results of using full graph message-passing for the TwoDOS channel model of (2) and Table I are shown in Fig. 3. The LDPC code used is a block length 10000, regular (3,30) code. This high-rate code is chosen so as to add only a small number of redundant parity bits. The SNR (E_b/N_0) is defined as the average signal energy divided by the noise power;

$$SNR = 10 \log_{10} \frac{\left(\sum_{n=0}^6 \binom{6}{n} (s_{n_0}^2 + s_{n_1}^2) \right) / 2^7}{R \cdot (2\sigma^2)}, \quad (8)$$

where s_{n_0}/s_{n_1} is the signal level given that the central bit is a 0/1 and has n nonzero neighbors and R is the LDPC code rate. From right to left the curves in Fig. 3 are; the uncoded

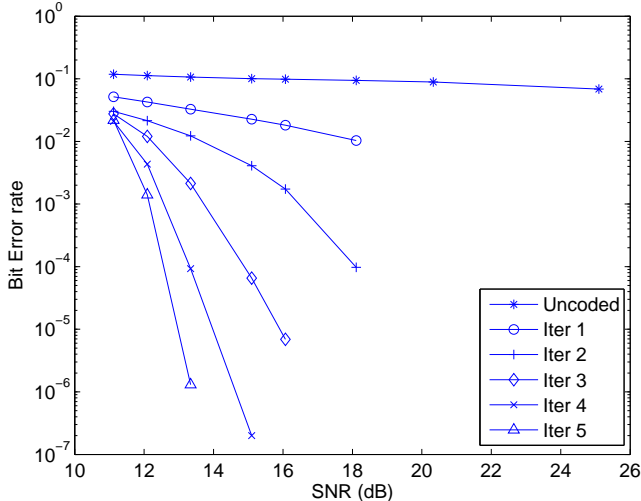


Fig. 3. Results of using the full graph message-passing algorithm for the TwoDOS recording model given by (2) and Table I.

performance, the performance of the full graph message-passing algorithm for a maximum of 1, 2, 3, 4, and 5 iterations. The number of iterations is kept low so as to reduce decoding delay. As the curves show, the improvement in performance is quite significant. The performance of the full graph algorithm after 5 iterations is about 8 dB better (at a bit error rate of 10^{-6}) than the performance reported in [9], where a stripe-wise Viterbi detector is used for the same ISI.

For the results shown here the full graph algorithm only takes into account the ISI from the nearest neighbors. Including the interference from the other shells, though computationally expensive, can still be accomplished at a significantly lower cost than the stripe-wise Viterbi detector where the complexity increases exponentially. Imminck *et al.*, [9] have proposed the use of modulation coding to eliminate data patterns that severely degrade the performance of the stripe-wise Viterbi detector. Furthermore, they have incorporated the modulation code and detection into a Bliss-like scheme. The modulation code can be incorporated seamlessly into our system model; the modulation code can be represented graphically and will add another level to the full graph. The connections of this subgraph will differ depending on whether the modulation code is incorporated in the usual way (after the LDPC encoder) or used in a Bliss-like scheme. We have not yet studied the performance of such a system.

IV. DENSITY EVOLUTION AND THRESHOLD COMPUTATION

For many channels and decoders of interest, LDPC codes exhibit a threshold phenomenon [12]; there exists a critical value of the channel parameter (noise tolerance threshold, say δ^*) such that an arbitrarily small bit error probability can be achieved if the noise level (δ) is smaller than δ^* and the code length is long enough. On the other hand, for $\delta > \delta^*$ the probability of bit error is larger than a positive

constant. Richardson and Urbanke [12] developed an algorithm called *density evolution* for iteratively calculating message densities, enabling the determination of the aforementioned threshold. Kavčić *et al.*, [13] extended the work of Richardson and Urbanke to compute noise tolerance thresholds for one-dimensional ISI channels.

Using a density evolution similar to that proposed by Kavčić *et al.*, [13] noise tolerance thresholds are computed for the full graph algorithm and the nonlinear TwoDOS channel. Following is a brief description of the algorithm. Density evolution tracks the “evolution” of the probability density function (pdf) of correct (or incorrect) messages passed on the graph as the iterations progress. Density evolution is described more conveniently using log-likelihood ratios (LLR) instead of probabilities to represent the messages. The LLR for the variable-to-check messages at the l th iteration is defined as $L_{x \rightarrow c}^{(l)} = \log \frac{\mu_{x \rightarrow c}^{(l)}(0)}{\mu_{x \rightarrow c}^{(l)}(1)}$. The LLRs $L_{c \rightarrow x}$, $L_{x \rightarrow r}$, and $L_{r \rightarrow x}$ are defined analogously. Using LLRs gives an equivalent representation of the full graph message-passing algorithm. Equations (3)-(6) can be rewritten as

$$\begin{aligned}
 L_{x \rightarrow c}^{(l)} &= \sum_{r \in N_r(x)} L_{r \rightarrow x}^{(l-1)} + \sum_{c' \in N_c(x) \setminus c} L_{c' \rightarrow x}^{(l-1)} \quad (9) \\
 \tanh\left(\frac{L_{c \rightarrow x}^{(l)}}{2}\right) &= (-1)^c \prod_{x' \in N(c) \setminus x} \tanh\left(\frac{L_{x' \rightarrow c}^{(l)}}{2}\right) \quad (10) \\
 L_{x \rightarrow r}^{(l)} &= \sum_{c \in N_c(x)} L_{c \rightarrow x}^{(l)} + \sum_{r' \in N_r(x) \setminus r} L_{r' \rightarrow x}^{(l-1)} \quad (11) \\
 L_{r \rightarrow x}^{(l)} &= F(L_{x' \rightarrow r}^{(l)}; x' \in N(r) \setminus x), \quad (12)
 \end{aligned}$$

The update for measured data-to-variable messages has no closed form when represented using LLRs. The “tanh” rule [14] cannot be applied to (6) since the measured data nodes are not binary-valued. Equation (12) represents the measured data-to-variable message update via a function F which performs the appropriate computation.

Let $f_v^{(l)}(x)$ be the pdf of the correct message from a variable node to a check node at the l th round of message-passing. This pdf is evolved through (9)-(12). The evolution of the density functions through (9) and (11) are simple convolutions and can be implemented efficiently using the fast Fourier transform. Density evolution for (10) can be implemented using the change in measure described in [12] or more efficiently by using a table-lookup as explained in [15]. For density evolution through (12) Monte Carlo simulations are used; message-passing is performed on the channel graph using a long block length and the pdf of the outgoing messages from the measured data nodes is approximated by using the histogram of computed messages.

After evolving $f_v^{(l)}(x)$ through (9)-(12), $f_v^{(l+1)}(x)$ is obtained. Using $f_v^{(l+1)}(x)$, the error probability at the $(l+1)$ th iteration, $p_e^{(l+1)}$, can be computed as

$$p_e^{(l+1)} = \int_{-\infty}^0 f_v^{(l+1)}(x) dx. \quad (13)$$

The noise tolerance threshold, δ^* , can be calculated as the supremum of all δ for which the error probability goes to zero as the iterations progress. Table II shows the computed thresholds for regular LDPC codes of different rates. The noise tolerance threshold is the variance of the AWGN. The SNR is calculated as in (8) except that the rate of the code is not taken into account. It should be noted that to compensate for the loss in density due to error-correction coding the bits need to be stacked closer, leading to increased ISI. This effect is not taken into account during the calculation of the thresholds for the different rate codes.

TABLE II
NOISE TOLERANCE THRESHOLDS FOR THE TwODOS CHANNEL.

LDPC Code	Code Rate	Threshold σ_*^2	Threshold SNR [dB]
(3,3)	0.000	0.0670	1.6070
(3,4)	0.250	0.0436	3.4729
(3,5)	0.400	0.0283	5.3499
(3,6)	0.500	0.0215	6.5433
(3,9)	0.667	0.0140	8.4064
(3,12)	0.750	0.0117	9.1859
(3,15)	0.800	0.0103	9.7393
(3,30)	0.900	0.0061	12.0144
(3,60)	0.950	0.0035	14.4270
(3,90)	0.967	0.0030	15.0965
(3,120)	0.975	0.0027	15.5541
(3,150)	0.980	0.0025	15.8883

In proving the existence of thresholds for memoryless channels the crucial innovation of Richardson and Urbanke [12] was the “concentration results.” These results state that as the block length tends to infinity the performance of the LDPC decoder on random graphs converges to its expected behavior and that the expected behavior can be determined from the corresponding cycle-free behavior. Kavčić *et al.*, [13] extended these concentration results to one-dimensional ISI channels by using LDPC coset codes.

For 2D ISI channels the concentration results do not hold since the channel graph has short cycles even in the limit of infinitely long block length. Hence existence of thresholds cannot be proved using the concentration analysis. However, our simulations seem to suggest that for the TwODOS channel the full graph algorithm respects the thresholds computed using density evolution. Simulations for long block lengths ($\sim 2 \times 10^6$) show that very low bit error rates ($\sim 10^{-6}$) are obtained only when the noise variance is smaller than the threshold. Although this does not prove the existence of a threshold, it suggests that the noise tolerance thresholds of Table II are upper bounds on the performance of the full graph algorithm. Besides that, the thresholds also serve as a design parameter; given a system with a specified SNR it is sufficient to pick an LDPC code having a smaller threshold SNR thereby ensuring that the bit-error rate can be made arbitrarily small as the block length increases.

V. CONCLUSION

A message-passing based scheme for joint equalization and decoding for nonlinear two-dimensional intersymbol interfer-

ence channels has been proposed. The scheme, called the full graph algorithm, performs sum-product message-passing on a joint graph of the error correction code and the channel. The complexity of the full graph algorithm is linear in the block length of the error correction code and quadratic in the size of interference neighborhood. The performance of the algorithm is studied for the two-dimensional optical storage paradigm. Simulations for the nonlinear channel model of TwoDOS show significant improvement over uncoded performance. The performance is about 8 dB better than that reported by Immink *et al.*, [9] for the same ISI. Using density evolution noise tolerance thresholds for the full graph algorithm are also computed.

VI. ACKNOWLEDGMENT

The authors would like to thank the reviewers for their helpful suggestions. This work was supported by the Office of Naval Research under Award N00014-03-1-0110.

REFERENCES

- [1] K. M. Chugg, X. Chen, and M. A. Neifeld, “Two-dimensional equalization in coherent and incoherent page-oriented optical memory,” *J. Opt. Soc. Amer. A*, vol. 16, pp. 549-562, Mar. 1999.
- [2] P. S. Kumar and S. Roy, “Two-dimensional equalization: theory and application to high density magnetic recording,” *IEEE Trans. Comm.*, vol. 42, pp. 386-395, Feb. 1994.
- [3] M. Marrow and J. K. Wolf, “Iterative detection of 2-dimensional channels,” *IEEE Info. Theory Workshop*, Paris, France, Mar. 2003.
- [4] O. Shental, A. J. Weiss, N. Shental, and Y. Weiss, “Generalized belief propagation receiver for near-optimal detection of two-dimensional channels with memory,” *IEEE Info. Theory Workshop*, San Antonio, Texas, Oct. 2004.
- [5] W. Weeks IV, “Full surface data storage,” Ph.D. thesis, University of Illinois at Urbana-Champaign, 1996.
- [6] N. Singla, J. A. O’Sullivan, R. S. Indeck, and Y. Wu, “Iterative decoding and equalization for 2-D recording channels,” *IEEE Trans. Magn.*, vol. 38, pp. 2328-2330, Sept. 2002.
- [7] Y. Wu, J. A. O’Sullivan, R. S. Indeck, and N. Singla, “Iterative detection and decoding for separable two-dimensional intersymbol interference,” *IEEE Trans. on Magn.*, 39(4):2115–2120, July 2003.
- [8] W. M. J. Coene, “Nonlinear signal-processing model for scalar diffraction in optical recording,” *Appl. Opt.*, vol. 42, No. 32, Nov. 2003.
- [9] A. H. J. Immink *et al.*, “Signal processing and coding for two-dimensional optical storage,” *Proc. GlobeComm.*, Piscataway, New Jersey, 2003.
- [10] A. Moinian, L. Fagoonee, B. Honary, and W. Coene, “Linear channel model for multilevel two dimensional optical storage,” *Proc. 7th Intl. Symp. Comm. Theory and Applications*, pp. 352-356, Ambleside, Lake District, UK, July 2003.
- [11] J. Riani, J. W. M. Bergmans, S. J. L. v. Beneden, W. M. J. Coene, and A. H. J. Immink, “Equalization and target response optimization for high density two-dimensional optical storage,” *Proc. 24th Symp. on Info. Theory in the Benelux*, pp. 141-148, May 2003.
- [12] T. Richardson and R. Urbanke, “The capacity of low-density parity-check codes under message-passing decoding,” *IEEE Trans. on Inform. Theory*, vol. 47, pp. 599-618, Feb. 2001.
- [13] A. Kavčić, X. Ma, and M. Mitzenmacher, “Binary intersymbol interference channels: Gallager codes, density evolution and code performance bounds,” *IEEE Trans. Inform. Theory*, vol. 49, pp. 1636-1652, July 2003.
- [14] F. R. Kschischang, B. J. Frey, and H. A. Loeliger, “Factor graphs and the sum-product algorithm,” *IEEE Trans. Inform. Theory*, vol. 47, pp. 498-519, Feb. 2001.
- [15] S.-Y. Chung, G. D. Forney, T. Richardson, and R. Urbanke, “On the design of low-density parity-check codes within 0.0045 dB of the Shannon limit,” *IEEE Comm. Letters*, vol. 5, pp. 58-60, Feb. 2001.